Canadian Conference - Pacific Conference on Earthquake Engineering 2023
Vancouver, British Columbia
June 25th – June 30th, 2023

Seismic Performance of a High-Rise Building Equipped with a Novel Semi-Active Variable Stiffness and Damping Actuator Subjected to Near-Field Ground Motions

Seyed Masoud Sajjadi Alehashem[1*], Ali Keyhani[2]

[1]Head of Civil & Structural Engineering Department, Tetra Consulting Engineers Company, Karaj, Alborz, Iran
[2]Assocciate Professor, Department of Civil Engineering, Shahrood University of Technology, Shahrood, Semnan, Iran
[*]masoud.sajjadi@yahoo.com (Corresponding Author)

ABSTRACT

Simulation studies of a high-rise (15-story) steel moment-resisting frame (MRF) building subjected to near-field ground motions were conducted, and the performance and efficacy of a novel semi-active variable stiffness and damping actuator in controlling the vibration responses of the building were evaluated. Near-field earthquake ground motions contain distinctive long-period velocity pulses, severely damaging structures within the near-field region. The proposed actuator is a hydro-pneumatic semi-active resettable device (HSRD) that includes a cylinder-piston assemblage comprising four separate chambers filled with two different materials, that is, magneto-rheological (MR) fluid and pressurized air. The two sides of a bypass pipe are connected to the two adjacent MR fluid chambers in the middle of the cylinder, forming a closed-circulating loop. The bypass pipe has an on−off valve controlling the stiffness by adjusting its on−off threshold and a functional valve controlling the damping by changing the MR fluid's property. The initial stiffness of HSRD is set by adjusting the pressures or lengths of the two gas chambers. Seismic responses of the building without and with the HSRD installed in all building's stories subjected to the near-field earthquake are simulated, and a series of semi-active control schemes were adopted to suppress the vibration responses of the building. The results confirm the ability of HSRD assisted by a semi-active control scheme for vibration mitigation of high-rise buildings subjected to near-field earthquakes.

Keywords: Seismic response, Semi-active control, Near-field earthquake, Variable stiffness, Variable damping.

INTRODUCTION

Near-field earthquake ground motions are characterized by a high-peak acceleration and a long-period velocity pulse together with a significant displacement component [1] that cause severe damage to buildings and other infrastructures, which are designed according to the current seismic codes. Hence, mitigating vibration due to near-field earthquakes is significant given the high life risks and economic losses. Many vibration mitigation techniques and devices have been developed to address the above setbacks, mainly categorized into passive, active, and semi-active groups.

Passive systems have been widely employed for vibration reduction applications; however, they operate in a narrow bandwidth around the designated tuned frequencies. Besides, as the peak ground acceleration or velocity of the near-field earthquake occurs in the form of a shock rather than a gradual building-up process, so passive dampers may not be able to dissipate seismic energy and prevent structures from severe damage quickly. On the other hand, active systems usually contain an actuator, following an appropriate control law and applying controlled force to guarantee vibration attenuation within a target frequency bandwidth. However, the active systems require a large amount of power consumption and may lead to instability of systems in case of control malfunction. Therefore, semi-active vibration mitigation devices have been advocated in real applications due to their additional damping feature and/or frequency-shift capability. The semi-active strategy is nearly identical to a conventional passive system except that the semi-active technique generates a variable coefficient of stiffness/damping, which can be adapted in real time according to different requirements. In other words, the semi-active vibration mitigation methods combine the advantages of passive and active control methods. In contrast, semi-active systems consume less power than active systems and have controllability over passive structures [2].

A resettable damper is among semi-active control systems as it only uses a small amount of energy to open and close a control valve. It can store the vibration energy and dissipate/release the stored energy at an appropriate moment by opening and closing the control valve at the proper times. The resettable device's control methods aim to find suitable moments for adjusting the stiffness and resetting the device by opening the control valve and increasing stiffness back to the high value by closing the control valve. Although vibration suppression is mainly achieved using a damping-adjustable mechanism rather than a stiffness-adjustable mechanism, the damping/stiffness-adjustable devices can provide large forces and have significant advantages for shock isolation purposes [3]. The concept of using an on-off semi-active hydraulic damper was first proposed by Kobori et al. [4]. The main idea is to manipulate the structural stiffness using resettable actuators in which each actuator behaves like a linear spring with different control schemes. In contrast to conventional viscous or rate-damping dampers, the force produced by the resettable dampers has no velocity dependence. Therefore, they are a perfect alternative to handle shock-type excitations such as near-field earthquake excitations. The capability of the resettable damper in shock isolation has already been testified [5]. Moreover, it is decentralized because the damper behavior only depends on the degree of freedom to which the damper is attached. The resettable damper is reliable and does not require full-state sensing, and its control laws are simple with minimal hardware complexity.

Furthermore, the control law does not require the exact model of the system; hence, it is robust to the uncertainty of the system's parameters [6]. There are two types of resettable devices, closed-form and open-form. The closed-form resettable devices usually consist of a double-acting cylinder-piston system with a bypass valve connecting two sides of the cylinder. They perform as hydraulic or pneumatic springs, resisting displacement in both directions. In addition, their un-stretchable spring length can be reset by releasing the working fluid or working gas from a high-pressure chamber to a low-pressure chamber through a bypass valve to absorb and dissipate the kinetic energy from the excited structure [7]. On the other hand, the open-form resettable devices use a two-chambered design with an independent control valve in each chamber without any bypass pipe. This approach treats each side of the piston as an independent chamber with its control valve and control command. In the open-form resettable device, the air is utilized as the working fluid, and the surrounding atmosphere acts as the fluid chamber. As a result, the device resists displacement in both directions, and its un-stretchable spring length can be reset by discharging the air to the surrounding atmosphere [8].

Although extensive numerical simulations and experimental studies were widely conducted to evaluate the vibration mitigation capability of resettable devices, only a few investigations have been devoted to implementing control approaches to high-rise buildings equipped with resettable devices against shock-type excitations or near-field earthquakes [9-11]. Even though the existing resettable devices have shown promising performance in handling shock-type loadings and near-field ground motions, they have some limitations in real applications. First, the damper's initial stiffness and damping capacity required by civil structures (e.g., multi-story buildings) are generally pretty large, challenging the performance of the current resettable dampers. Second, in both types of resettable dampers, the damper's initial stiffness is not adjustable, and to satisfy the design requirements, perforce, a new damper with different geometry must be fabricated to achieve a higher initial stiffness. Third, the damping capacity of both types of resettable dampers is limited, especially when the damper encounters a significant displacement excitation. Furthermore, in both types of resettable dampers, the initial stiffness of the damper is highly sensitive to the piston position at the moment of completing the device installation. Any dislocation of the piston from the central point of the cylinder to either side would cause unequal stiffness in two directions. Since the air with atmospheric pressure is used as working fluid in the open-form resettable damper, increasing the damper's initial stiffness by boosting the gas pressure is impossible. It is commonly doable by fabricating a new damper with a larger cross-section cylinder. On top of that, discharging and sucking the air from the surrounding atmosphere may not be feasible in an actual application where the dampers usually are covered or sealed.

To take advantage of the resettable dampers in handling shock-type loadings and near-field earthquakes while overcoming the shortages of the current resettable devices as mentioned above, a novel concept of the hydro-pneumatic semi-active resettable device (HSRD) has been proposed and realized by the authors [12] through experimental verification on the force–displacement relationship of an HSRD prototype. The proposed device consists of a cylinder-piston system containing four separate chambers filled with two different types of materials (i.e., the MR fluid and pressurized air) and a bypass pipe with an on-off valve having a changeable opening threshold and a functional valve for changing MR fluid property. The two sides of the bypass pipe are connected to the MR fluid chambers in the middle of the chamber, forming a closed-circulating loop with the two valves controlling stiffness and damping. The pressurized air is filled in the two gas chambers at two opposite ends of the chamber. MR fluid belongs to a broader group of 'intellectual' materials with variable damping properties when exposed to a changeable external magnetic field [13]. The pressurized air plays the role of spring. When the on-off control valve is closed, the device serves as a spring element, of which the bulk modulus of the pressurized gas provides the stiffness. Energy dissipation occurs when MR fluid flows through the functional valve called MR-valve. The MR-valve is an electric coil controlling the MR fluid's viscosity by applying a controllable magnetic field to a narrow gap where the MR fluid is pushed to pass through due to the pressure difference between the right and left chambers. In the authors' previous study [14], simulation studies with a low-rise (5-story) and a mid-rise (10-story) building structures subjected to three near-field earthquakes were conducted to evaluate the performance of HSRD. Three semi-active control schemes are considered to create optimal hysteresis loops of HSRD for achieving prominent vibration mitigation. It is revealed that the device with all the control schemes is effective in vibration suppression of the structures suffering from near-field earthquakes. The present study explores the performance of HSRDs for vibration mitigation of a high-rise (15-story) building structure subjected to near-field earthquakes.

PROPOSED HYDRO-PNEUMATIC SEMI-ACTIVE RESETTABLE DEVICE

The configuration and working mechanism of the HSRD

The proposed resettable device consists of a cylinder-piston structure, a bypass pipe with its two ends connected to the cylinder, and an on-off control valve together with an MR-valve mounted on the pipe. The HSRD structure is depicted in Figure 1. The cylinder has four chambers filled with viscous intelligent material and pressurized gas, entirely separated by a movable piston embedded within the cylinder. The pressurized gas performs as a spring. The initial stiffness of the proposed device can be adjusted by changing either the gas pressure or the initial length of the gas chamber. Air is employed as the working gas for being pressurized in the cylinder. MR fluid is chosen as working fluid because of its high energy-dissipation rate during circulating in the cylinder-pipe loop when the MR-valve applies a magnetic field. Specifically, MR fluid is a controllable fluid that quickly responds to an applied magnetic field with a dramatic change in its rheological behavior. MR fluid's essential characteristic is the ability to change reversibly from a free-flowing viscous liquid to a semi-solid material, yielding a controllable yield strength in milliseconds when exposed to a magnetic field [15]. This fast shift leads to a significant change in the resistive force of the device and thus causes a large amount of energy dissipation in a very short time. This device's initialization is conducted by changing either the gas pressure or the initial length of the gas chamber to adjust the stiffness. After initialization, the valves are closed, and the input energy is stored in the pressurized gas. By automatically opening the control valve (resetting the device) at a due moment, the stored potential energy in the pressurized gas is released, pushing the viscous material to flow across the MR-valve to another side of the cylinder because of the pressure difference. Meanwhile, by applying an electrical current to MR-valve, a magnetic field is applied to the passing-by MR fluid. The magnetic field adjusts MR fluid's shear yield stress in few milliseconds, thereby dissipating a large amount of stored energy as heat. The device damping can be adapted in real time by changing the electric current input to the MR-valve. This configuration and working mechanism of the proposed resettable device mainly facilitates the effective control action and manipulates the device's hysteresis behavior by setting the control valve's threshold and automatically controlling both the control valve and the MR-valve. By resetting the resettable device, the hysteresis loop of the HSRD can cover all four quadrants in the force-displacement diagram and thus results in more energy dissipation. Therefore, the proposed device's stiffness, damping, and hysteresis behavior can be independently adjusted. Besides, HSRD is "fail-safe" since the device serves as an ordinary passive damper when the on-off valve and/or MR-valve fails.

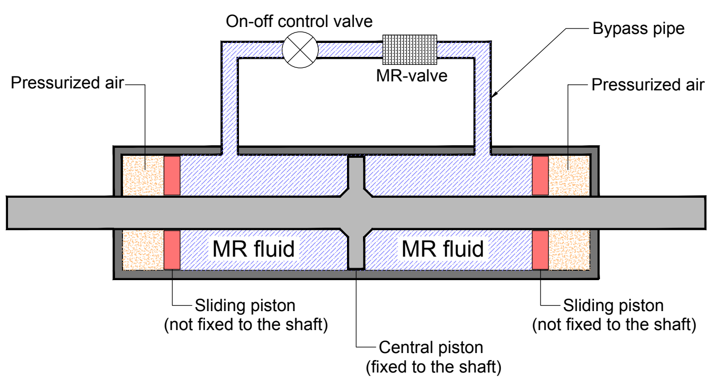

Figure 1. Schematic of the proposed HSRD.

Mechanical behavior of the HSRD

A force-displacement relationship of the proposed device is formulated in the authors' previous work [12] to develop a linear model representing the device's stiffness change and pressure drop. When the control valve is closed, the gas chamber volume in each chamber related to the piston displacement leads to a change in the resistive force. In the proposed HSRD, both the pressurized gas and MR fluid resist piston movement. To achieve the linear force–displacement relationship of HSRD, the length of the air cylinder (L_{0G}) is designed two times the predictable inter-story drift of each story of the building to be controlled so that the condition of $x < 0.5L_{0G}$ which is essential for linear force-displacement relationship assumption is always satisfied [12]. With this setting, the linear force–displacement relationship of HSRD is given by [12]:

$$F_G(x) = -\frac{2A^2\gamma p_{0G}}{V_{0G}}x \tag{1}$$

where A is the piston cross-section area, γ the heat ratio of gas, p_{0G} the initial gas pressure, V_{0G} the initial volume of the gas chamber, and x the central piston displacement. The effective stiffness of the pressurized gas, k_G, is derived from Eq. (1) as:

$$k_G = \frac{2A^2\gamma p_{0G}}{V_{0G}} \tag{2}$$

If MR fluid is considered as a compressible liquid, then the resistive force and the MR fluid's stiffness depend on the bulk modulus. For many fluids, the pressure–volume relationship is linear and characterized by a proportionality constant called the bulk modulus, κ. An increment in pressure results in a decrement in volume. Considering the pressure change in MR fluid on both sides of the piston, the resistive force of MR fluid is given by [12]:

$$F_{MR}(x) = \frac{2\kappa A^2}{V_{0MR}}x \tag{3}$$

and similarly, the effective stiffness of MR fluid becomes:

$$k_{MR} = \frac{2\kappa A^2}{V_{0MR}} \tag{4}$$

In the proposed HSRD, the MR fluid and pressurized air work as two springs connected in series. Hence, the total stiffness of the device, k_d, is:

$$k_d = \frac{k_G k_{MR}}{k_G + k_{MR}} \tag{5}$$

As the bulk compressibility modulus κ is very large for MR fluid, the MR fluid stiffness is much bigger than the gas stiffness ($k_{MR} \gg k_G$), and the device stiffness can be approximately written as a function of the stiffness of the gas:

$$k_d \cong k_G \tag{6}$$

Rewriting Eq. (2) in terms of the device's geometry leads to a linear stiffness of the device as:

$$k_d = k_G = \frac{2(\pi D^2/4 - A_s)^2\gamma p_{0G}}{[(\pi D^2/4 - A_s)L_{0G} + V_{con}]} \tag{7}$$

where k_d is the stiffness of the HSRD, D is the central piston diameter, and A_s is the shaft cross-section area. L_{0G} is the initial length of the gas chambers, which can be initially set to different values by setting the sliding pistons' position in accordance with the damper's initial stiffness determined by the seismic design demand. V_{con} is the constant volume in the air chambers (e.g., the air volume trapped in the voids at cylinder caps, etc.).

The MR-valve performs as an energy dissipation adapter in the proposed HSRD (Figure 1). Once the HSRD is excited, the device's resistive force can be measured by a load cell (as shown in Figure 3). At the resetting time, when the resistive force is maximum, the controller commands to open the control valve, thereby pushing the MR fluid across the MR-valve (in the flow mode) due to the pressure difference between the two sides of the cylinder. At the same time, the controller calculates the required yield stress of MR fluid according to the measured resistive force of the device. Then, by altering the magnetic field in the MR-valve, the yield stress can be adjusted to its threshold value continuously until most of the stored energy in the HSRD is dissipated by shearing the activated MR fluid and the device's resistive force returns to zero. Afterward, the magnetic field is set to zero (MR fluid flows in off-state), and the device waits for the next resetting time. All these processes happen in few milliseconds. Using the MR-valve as an energy dissipator with a relatively large and fast energy dissipation capacity in the proposed HSRD is another advantage of HSRD over the other resettable devices.

CONTROL SCHEMES AND ANALYTICAL MODEL

There are three primary control schemes based on the control valve's commands. In the first control scheme (called resetting control), the control valve opens for a short time at the peaks of the central piston displacement (when the piston velocity is zero). As a result, practically all stored energy is released and dissipated abruptly. For a sinusoidal piston displacement, Figure 2(a) illustrates the behavior of the HSRD when the resetting control is implemented, with the assumption that all stored energy is released at the peak of each sine wave. Further examination of Figure 2(a) reveals that the resetting control method provides a damping effect in all four quadrants of the force-displacement diagram. In the second control scheme (called switching control type-1), the valve is opened at the peaks of the central piston displacement. It remains in the open status until the central piston returns to the initial zero position. The force–displacement curve in this scheme is shown in Figure 2(b) for a sine wave input. Finally, in switching control type-2 (Figure 2(c)), the valve is opened at the zero position. It remains in the open status until the central piston reaches peak displacements and then closes and resists the central piston displacement. It is worth noting that for a linear single-degree-of-freedom structure equipped with a resettable device, the switching control type-2, in which the damping force is added to the system only in the second and fourth quadrants, does not increase the total base shear force in comparison with the other two control schemes [16]. This is significant merit since increasing the foundation demand is undesirable or potentially damaging.

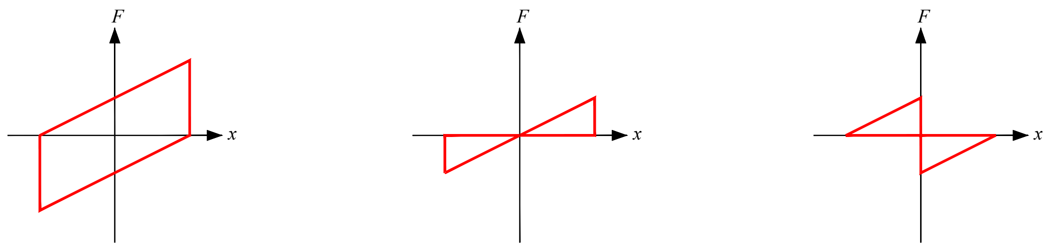

(a) Resetting control *(b) Switching control type-1* *(c) Switching control type-2*

Figure 2. Schematic of three control schemes for HSRD.

The semi-active control strategies are decentralized with the least uncertainty involved. To execute a control command to each HSRD deployed on a building, we need only local measurements, e.g., the real-time damper resistive force (compressive force in each direction) and velocity of the central piston, as shown in Figure 3(b). The resistive force of the HSRD can be measured by a load cell (e.g., piezo-resistive force sensor) located between one end of the HSRD's shaft and the fixture bracket, as shown in Figure 3(b). The velocity of the central piston can be measured directly by a velocity meter (e.g., LVT sensor) connected to the other end of the HSRD's shaft. The structure's mass and stiffness properties do not explicitly affect the control schemes. Thus, the control law is highly robust in regard to modeling errors in the mass and stiffness properties of the structure or nonlinearity that may occur to the structure. In the following, these three control schemes will be compared with the uncontrolled structure (without any damper installed in the building) for performance assessment of HSRD.

A model of a multi-story shear-type frame equipped with HSRDs in its bracing system is shown in Figure 3(a), where the HSRDs and the bracing system work as two springs in series, and they are connected in parallel with the shear-type frame. If k_{bi} denotes the horizontal stiffness of the asymmetric bracing in the *i*th story, then the effective stiffness of the entire HSRD–bracing system in the *i*th story, denoted as k_{hi}, is given by:

$$k_{hi} = \frac{k_{di} k_{bi}}{k_{di} + k_{bi}} \tag{8}$$

where k_{di} is the stiffness of the HSRD, as defined in Eq. (7). If the bracing system stiffness is remarkably larger than the HSRD stiffness ($k_{bi} \gg k_{di}$), then the stiffness of the HSRD–bracing system can be considered approximately equal to HSRD stiffness $k_{hi} \cong k_{di}$. It assumes that k_{bi} is large enough so that we can use $k_{hi} \cong k_{di}$ in simulation. The k_{di} is assumed proportional to the story stiffness, k_i. Three different stiffness ratios, namely, $k_{di}/k_i = 0.25$, $k_{di}/k_i = 0.5$, and $k_{di}/k_i = 1$, are considered in the subsequent simulation studies.

The HSRDs described above operate in semi-active mode. The control valve can be opened for the semi-active control operation with appropriate commands, and the three control schemes explained above are employed to provide the control commands. The equilibrium of forces acting on each story of the building is obtained (Figure 3(c)) to develop a set of linear state-space equations representing an *n*-story building equipped with HSRDs.

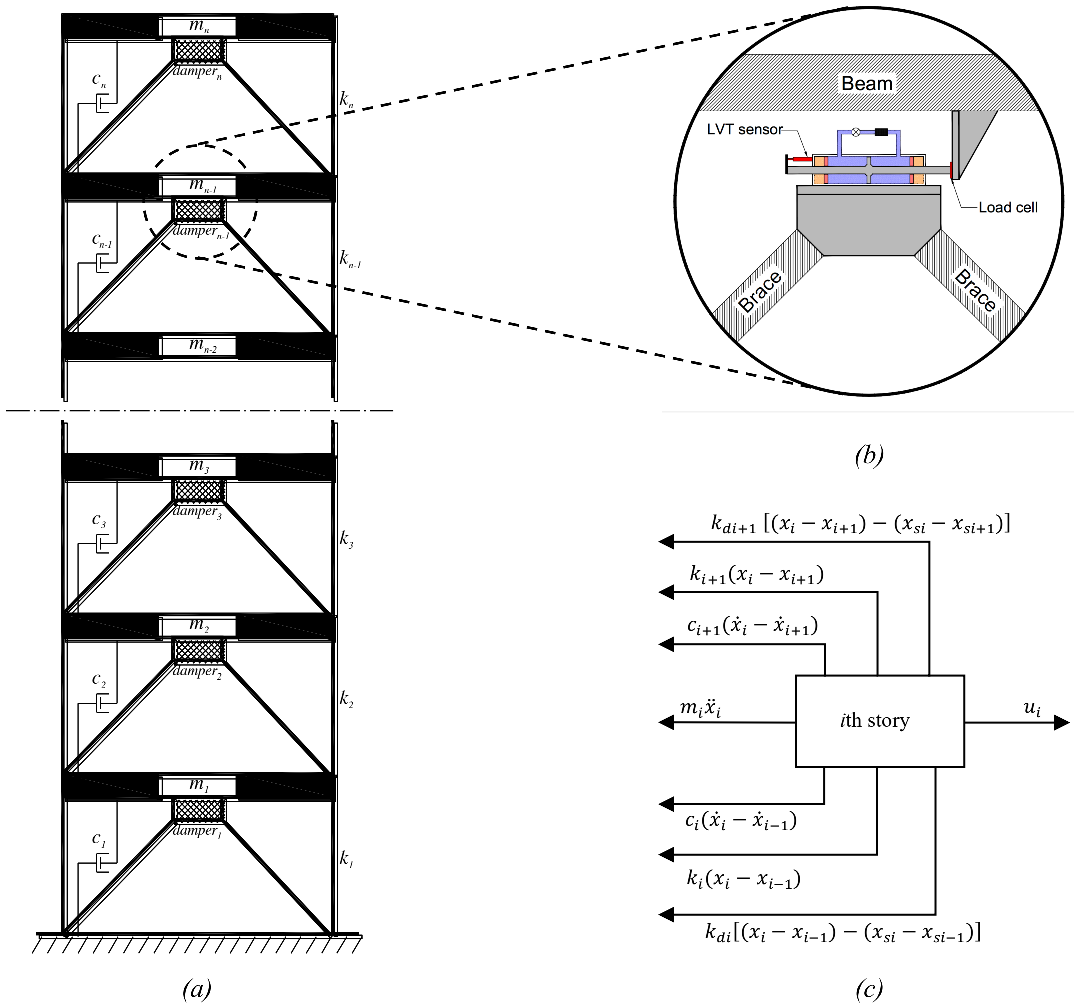

Figure 3. A model of building structure equipped with HSRDs: (a) A multi-story frame with HSRDs installed in the bracing system, (b) Damper and sensors installation details, and (c) Equilibrium of forces acting on the ith story.

The governing equation for the ith story is given as:

$$\begin{gathered} m_i\ddot{x}_i - c_i\dot{x}_{i-1} + (c_i + c_{i+1})\dot{x}_i - c_{i+1}\dot{x}_{i+1} \\ -k_i x_{i-1} + (k_i + k_{i+1})x_i - k_{i+1}x_{i+1} \\ -k_{di}x_{i-1} + (k_{di} + k_{di+1})x_i - k_{di+1}x_{i+1} \\ -k_{di}(x_{si} - x_{si-1}) + k_{di+1}(x_{si+1} - x_{si}) = u_i \end{gathered} \tag{9}$$

where k_{di} is the stiffness of the HSRD–bracing system, x_{si} is the central piston's position of the HSRD deployed in the ith story, and $u_i = -m_i\ddot{x}_g$ is the equivalent earthquake load acting on the ith floor ($\ddot{x}_g$ is the earthquake-induced ground acceleration). The resistive force of the HSRD in the ith story is given by:

$$F_{di} = k_{di}[(x_i - x_{i-1}) - (x_{si} - x_{si-1})] \tag{10}$$

At the resetting time (when the control valve is commanded to be opened), the relative displacement of the HSRD piston is set to be equal to the inter-story displacement of the ith story:

$$(x_{si} - x_{si-1}) = (x_i - x_{i-1}), \textit{ HSRD is reset} \tag{11}$$

Hence, the resistive force of the HSRD is set to zero. As a result, a state-space representation of the multi-story building is obtained as:

$$\dot{z}(t) = \mathbf{A}z(t) + \mathbf{B}u(t)$$
$$\mathbf{A}_{2\mathrm{n}\times 2\mathrm{n}} = \begin{bmatrix} \mathbf{0}_{\mathrm{n}\times\mathrm{n}} & \mathbf{I}_{\mathrm{n}\times\mathrm{n}} \\ -\mathbf{M}^{-1}(\mathbf{K}+\mathbf{K}_{\mathrm{d}})_{\mathrm{n}\times\mathrm{n}} & -\mathbf{M}^{-1}\mathbf{C}_{\mathrm{n}\times\mathrm{n}} \end{bmatrix}$$
$$\mathbf{B}_{2\mathrm{n}\times(\mathrm{n}+1)} = \begin{bmatrix} \mathbf{0}_{\mathrm{n}\times 1} & \mathbf{0}_{\mathrm{n}\times\mathrm{n}} \\ -\mathbf{Ir}_{\mathrm{n}\times 1} & -\mathbf{M}^{-1}\mathbf{K}_{\mathrm{ds}\,\mathrm{n}\times\mathrm{n}} \end{bmatrix} \tag{12}$$
$$u(\mathrm{t}) = \begin{bmatrix} \ddot{x}_g \\ x_{s_{drift}} \end{bmatrix}$$

where $\mathbf{M}$, $\mathbf{C}$, and $\mathbf{K}$ are the building mass, damping, and stiffness matrices, respectively. $\mathbf{K}_{\mathrm{d}}$ is the stiffness matrix of the HSRD–bracing system, and it is proportional to the building stiffness. $x_{s_{drift}}$ is the vector of relative displacements of two ends of the central piston of the HSRDs in different stories, and $\mathbf{K}_{\mathrm{ds}}$ is the effective stiffness matrix of the HSRDs installed in different stories of the building, which is defined as:

$$\mathbf{K}_{\mathrm{ds}} = \begin{bmatrix} -k_{d1} & k_{d2} & & & & & \\ & -k_{d2} & k_{d3} & & & & \\ & & \ddots & \ddots & k_{di} & & \\ & & & & -k_{di} & k_{di+1} & \\ & & & & & \ddots & \ddots & k_{dn} \\ & & & & & & & -k_{dn} \end{bmatrix} \tag{13}$$

where the elements of $\mathbf{K}_{\mathrm{ds}}$ are zero except for $\mathbf{K}_{\mathrm{ds}}(i,i) = -k_{di}$ and $\mathbf{K}_{\mathrm{ds}}(i-1,i) = k_{di}$.

SIMULATION RESULTS

The studied building is a steel moment-resisting-frame (MRF) structure with intermediate ductility, designed according to the Iranian Code of Practice for Seismic Resistant Design of Buildings (Standard No. 2800) [17]. The building site is located in a very high-intensity near-field seismic zone on soil type II (based on the soil and site categories of the code). These building structures satisfied all seismic design criteria based on the Iranian Code of Practice for Seismic Resistant Design of Buildings [17]. The studied building frames each have three bays, with each bay being 6 m in length and the height of each story being 3.2 m. The HSRDs are installed at the middle bay of the building frames on each floor of a 15-story building, as shown in Figure 3(a). The buildings are shear-type frame structures. The fundamental period of the 15-story building is 2.5 sec. The structural properties of the building are presented in Table 1. Damping in each mode is assumed to be proportional to the modal frequency and restricted to 10% of the critical damping at any vibration mode. The damping in the first mode is assumed $\xi_1 = 2\%$. Therefore, the damping in the *i*th mode is given by $\xi_i = \min\left\{\frac{0.02}{\omega_1}\omega_i, 0.1\right\}$, where ω_i is the natural vibration frequency of the *i*th mode. The damping matrix $\mathbf{C}$ is determined with the postulation of modal damping via the following expression:

$$\mathbf{C} = \mathbf{M}\Phi \begin{bmatrix} 2\xi_1\omega_1 & & & & \\ & \ddots & & & \\ & & 2\xi_i\omega_i & & \\ & & & \ddots & \\ & & & & 2\xi_n\omega_n \end{bmatrix} \Phi^{-1} \tag{14}$$

where Φ is the mode shape matrix (i.e., the eigenvectors of $\mathbf{M}^{-1}\mathbf{K}$) and the omitted entries in the matrix are all zero.

Table 1. Properties of the 15-story building.

story	1	2	3	4	5	6	7	8	9	10	11	12	13	14	15
m_i (ton)	78.1	77.6	76.8	76.4	76.3	76.1	75.6	75.5	75.0	74.6	74.3	73.6	73.3	72.8	71.6
k_i (kN/m)	97426	53020	51782	50833	49983	48625	40409	34511	34511	32319	32319	25459	22266	16955	11805

For the HSRD installed in each story, its stiffness can be described in terms of story stiffness ratio. Here, three different stiffness ratios, namely, $k_{d\,i} = 0.25k_i$, $k_{d\,i} = 0.5k_i$, and $k_{di} = k_i$, are considered to evaluate the effect of the HSRD's stiffness on the seismic response of the buildings. The three historical near-field ground motions of the SAC Steel Project [18] are adopted to assess the performance of the HSRDs against near-field earthquakes. The chosen near-field earthquake are Kobe-Takatori station (KB95tato), Loma Prieta-Los Gatos station (LP89lgpc), and Northridge-Olive View station (NR94sylm) with their peak ground acceleration (PGA) scaled to 0.35g are utilized as the excitation input to the buildings. MATLAB™/Simulink™ is used to simulate the responses of the buildings undergoing different input excitations. The numerical results for the building subjected to the three near-field earthquakes are obtained to evaluate the performance of each control scheme. Evaluation criteria are peak response quantities of each story at the device–floor connecting points, including the story displacement, inter-story drift, RMS story acceleration, and story shear force. The RMS story acceleration response represents the comfort of tenants over the entire response, which is defined by $a_{\mathrm{RMS}} = \sqrt{\sum_{i=1}^{n} a_i^2 \cdot {}^{\Delta t}/_{T}}$.

The numerical simulation results of peak responses of the 15-story building are listed in Table 2. All quantities are normalized by dividing them by the corresponding values of the uncontrolled structures. It is observed from the table that all three semi-active control strategies demonstrate their effectiveness in reducing peak displacement ($\mathrm{x_{max}}$). Similarly, with the semi-active control schemes, the peak inter-story drift ($\mathrm{Drift_{max}}$) is reduced compared to the uncontrolled case in Table 2. The decrement level is increased by raising the ratio $\mathrm{k_{di}/k_i}$ but with different values under the three earthquakes.

For all three earthquakes, the maximum reduction in inter-story drift is achieved by the resetting control method. A decrease of about 33%-62%, as a function of the k_{di}/k_i ratio, is witnessed in the resetting control under different earthquakes. The switching control type-1 generates a maximum reduction of about 5%-49% in terms of inter-story drift, depending on the ratio k_{di}/k_i and earthquake scenario. The switching control type-2 produces a decrement ratio of about 14%-48% under different earthquakes.

All three semi-active control methods effectively decrease the RMS story acceleration (a_{RMS}). The reduction is proportional to the ratio of k_{di}/k_i. The maximum decrement of the RMS is observed in the resetting control method, with about 37%-66% reduction during the three earthquakes. Similarly, the switching control type-1 and switching control type-2 methods generate 15%-49% and 29-54% decrement in RMS story acceleration, respectively.

Although the HSRDs add stiffness to the stories through the bracing system, the buildings' base shear force does not increase when resetting control and switching control type-2 are adopted. As shown in Table 2, in most cases, these two semi-active control strategies decrease the base shear force (V_{b}) compared to the uncontrolled structures under different earthquakes. The maximum decrement of base shear force (V_{b}) is observed in the switching control type-2, with about 15%-46% reduction during the three earthquakes. Similarly, the resetting control method produces a decrement ratio of about 11%-41% under different earthquakes.

The peak inter-story drift is illustrated in Figure 4. As shown in the figure, the three semi-active control strategies effectively decrease the inter-story drift of all stories under the three earthquakes. The best performance is observed when executing the resetting control method.

The RMS story acceleration is portrayed in Figure 5. It can be observed that the three control strategies perform similarly in reducing the RMS response under all three earthquakes. The response reduction is increasingly prominent in higher stories.

Figure 6. depicts the story shear force under different earthquakes. Both resetting control and switching control type-2 reduce the story shear force under the three earthquakes. However, the reduction is more significant in switching control type-2 in Kobe and Loma Prieta earthquakes.

Table 2. Peak responses of the 15-story model.

Earthquake	Control Scheme	x_{max} (m)	$\frac{x_{max}^{con}}{x_{max}^{unc}}$	$Drift_{max}$ (m)	$\frac{Drift_{max}^{con}}{Drift_{max}^{unc}}$	a_{RMS} (m/s²)	$\frac{a_{RMS}^{con}}{a_{RMS}^{unc}}$	V_b (kN)	$\frac{V_b^{con}}{V_b^{unc}}$
Kobe (KB95tato)	$k_{di} = 0.25k_i$								
	Resetting control	0.597	0.66	0.051	0.67	1.91	0.63	2779.7	0.83
	Switching control type-1	0.872	0.97	0.073	0.95	2.56	0.85	3654.0	1.09
	Switching control type-2	0.705	0.78	0.061	0.80	2.14	0.71	2844.5	0.85
	Uncontrolled	0.903	---	0.077	---	3.02	---	3346.1	---
	$k_{di} = 0.5k_i$								
	Resetting control	0.490	0.54	0.045	0.58	1.62	0.54	2627.1	0.79
	Switching control type-1	0.807	0.89	0.068	0.88	2.42	0.80	3757.5	1.12
	Switching control type-2	0.591	0.65	0.058	0.75	1.87	0.62	2392.1	0.71
	Uncontrolled	0.903	---	0.077	---	3.02	---	3346.1	---
	$k_{di} = k_i$								
	Resetting control	0.407	0.45	0.036	0.48	1.40	0.46	2990.2	0.89
	Switching control type-1	0.668	0.74	0.056	0.73	2.25	0.75	4167.2	1.25
	Switching control type-2	0.495	0.55	0.053	0.69	1.64	0.54	2301.4	0.69
	Uncontrolled	0.903	---	0.077	---	3.02	---	3346.1	---
Loma Prieta (LP89lgpc)	$k_{di} = 0.25k_i$								
	Resetting control	0.729	0.73	0.062	0.67	1.79	0.54	3118.8	0.74
	Switching control type-1	0.888	0.88	0.074	0.80	2.26	0.68	3261.2	0.78
	Switching control type-2	0.928	0.92	0.079	0.86	2.28	0.69	3430.8	0.82
	Uncontrolled	1.004	---	0.093	---	3.30	---	4188.6	---
	$k_{di} = 0.5k_i$								
	Resetting control	0.575	0.57	0.050	0.54	1.60	0.49	3148.9	0.75
	Switching control type-1	0.800	0.80	0.067	0.73	1.97	0.60	3426.5	0.82
	Switching control type-2	0.852	0.85	0.075	0.81	1.95	0.59	3217.8	0.77
	Uncontrolled	1.004	---	0.093	---	3.30	---	4188.6	---
	$k_{di} = k_i$								
	Resetting control	0.427	0.43	0.037	0.39	1.37	0.42	3366.6	0.80
	Switching control type-1	0.669	0.67	0.057	0.62	1.83	0.56	3640.0	0.87
	Switching control type-2	0.689	0.69	0.064	0.69	1.83	0.55	2824.5	0.67
	Uncontrolled	1.004	---	0.093	---	3.30	---	4188.6	---
Northridge (NR94sylm)	$k_{di} = 0.25k_i$								
	Resetting control	0.445	0.55	0.036	0.51	1.31	0.47	1927.4	0.63
	Switching control type-1	0.616	0.76	0.055	0.78	1.99	0.72	2759.4	0.90
	Switching control type-2	0.641	0.79	0.055	0.77	1.82	0.66	2286.2	0.74
	Uncontrolled	0.813	---	0.071	---	2.78	---	3076.1	---
	$k_{di} = 0.5k_i$								
	Resetting control	0.400	0.49	0.033	0.47	1.12	0.40	1835.6	0.60
	Switching control type-1	0.510	0.63	0.044	0.63	1.69	0.61	2768.9	0.90
	Switching control type-2	0.567	0.70	0.048	0.68	1.57	0.57	1963.4	0.64
	Uncontrolled	0.813	---	0.071	---	2.78	---	3076.1	---
	$k_{di} = k_i$								
	Resetting control	0.323	0.40	0.027	0.38	0.95	0.34	1818.5	0.59
	Switching control type-1	0.429	0.53	0.036	0.51	1.40	0.51	2581.5	0.84
	Switching control type-2	0.453	0.56	0.038	0.54	1.28	0.46	1660.7	0.54
	Uncontrolled	0.813	---	0.071	---	2.78	---	3076.1	---

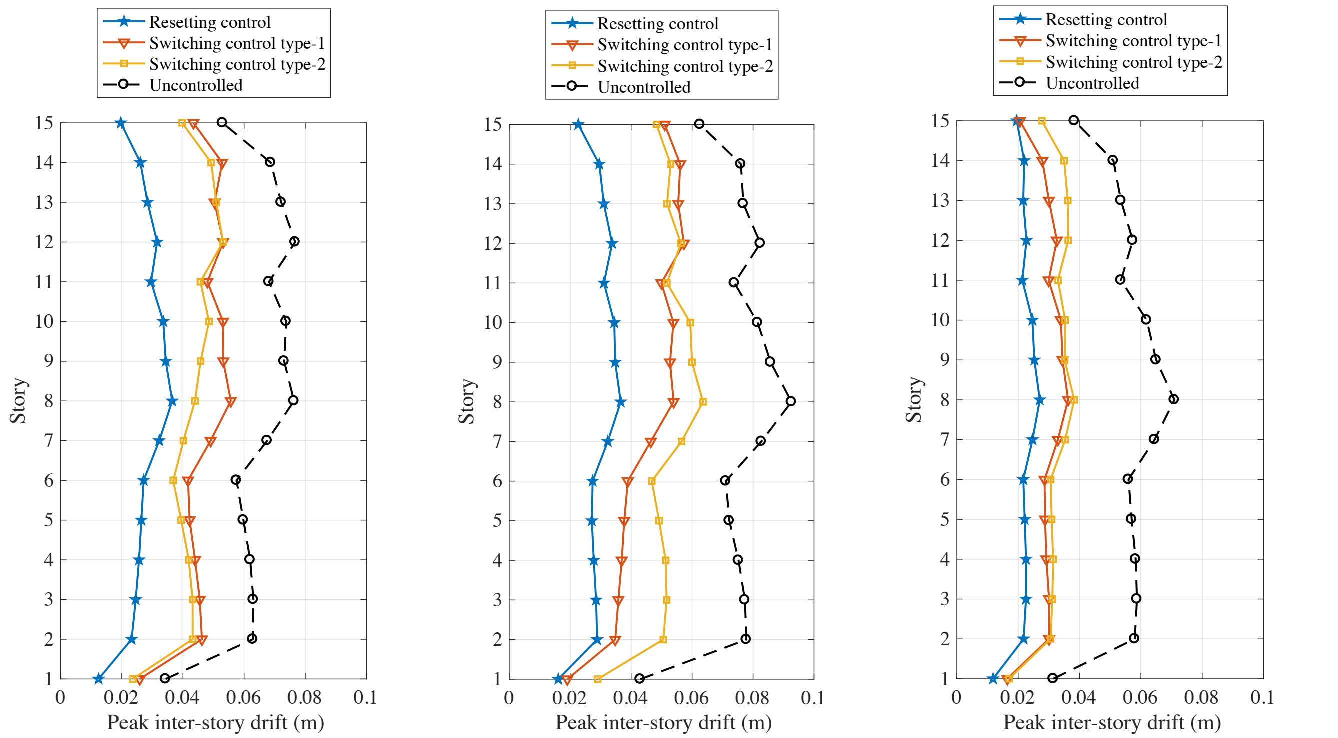

(a) Kobe (KB95tato) *(b) Loma Prieta (LP89lgpc)* *(c) Northridge (NR94sylm)*

Figure 4. Peak inter-story drift of the 15-story structure equipped with five HSRDs ($k_{di} = k_i$).

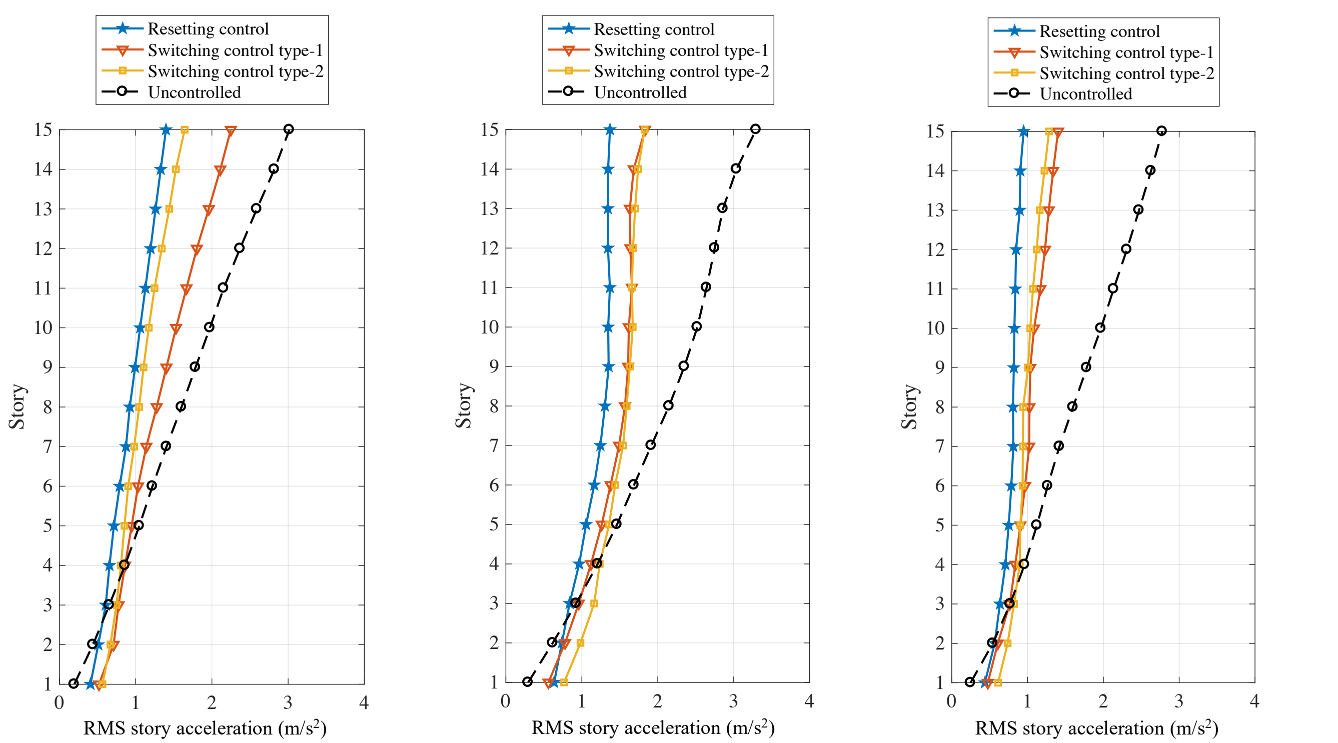

(a) Kobe (KB95tato) *(b) Loma Prieta (LP89lgpc)* *(c) Northridge (NR94sylm)*

Figure 5. RMS story acceleration of the 15-story structure equipped with five HSRDs ($k_{di} = k_i$).

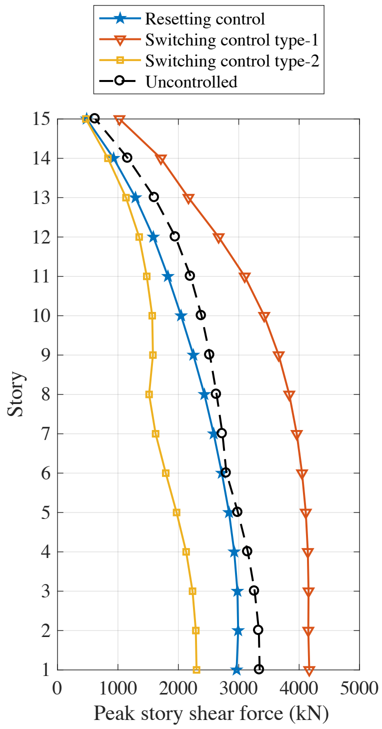

(a) Kobe (KB95tato)

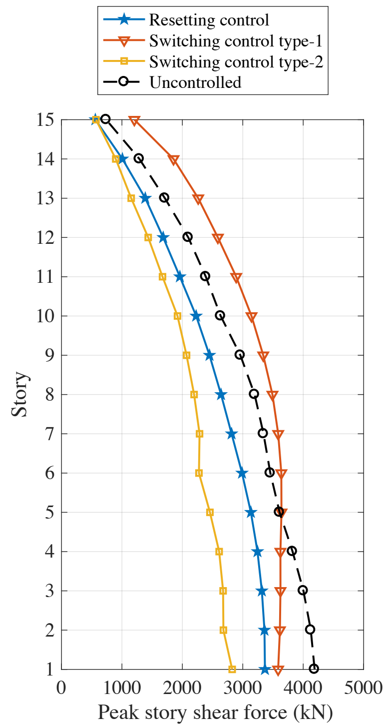

(b) Loma Prieta (LP89lgpc)

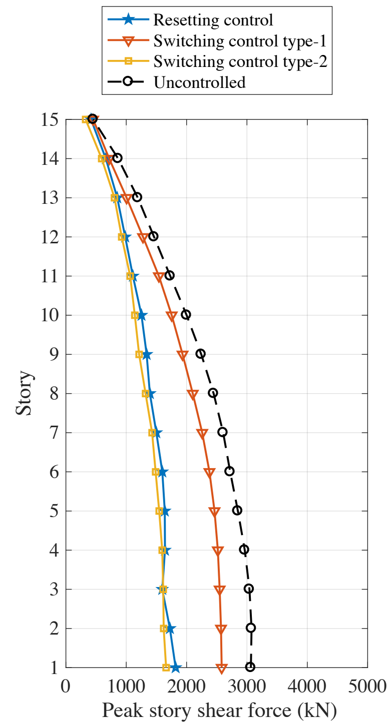

(c) Northridge (NR94sylm)

Figure 6. Story shear force of the 15-story structure equipped with five HSRDs ($k_{di} = k_i$).

CONCLUSIONS

A novel semi-active variable stiffness and damping actuator was proposed for vibration control of high-rise buildings subjected to near-field earthquakes. The mechanical behavior of the proposed hydro-pneumatic semi-active resettable device (HSRD) was analytically formulated. To investigate the effectiveness of the proposed HSRDs in controlling the seismic response of the buildings against near-field earthquakes, the seismic response of a 15-story building was numerically simulated under three near-field earthquakes, where the PGAs of the near-field earthquakes were scaled to 0.35g. Three semi-active control strategies, namely, resetting control, switching control type-1, and switching control type-2, were implemented to control the HSRDs. A comparative study was conducted between the semi-active control schemes and the uncontrolled case. The following results were revealed:

- With the aid of the provided semi-active control schemes, the seismic response level of the 15-story building equipped with HSRDs is distinctly lower than that of the uncontrolled case in terms of peak displacement, peak inter-story drift, and RMS story acceleration. This validates the capability of the proposed HSRD in mitigating the seismic response of high-rise buildings subjected to near-field earthquakes;
- The decrements in peak inter-story drift are different when using different semi-active control approaches. However, the performance of all semi-active control methods increases by raising the $k_{d\,i}/k_i$ ratio. Also, the decrements in RMS story accelerations were proportional to ratios of $k_{d\,i}/k_i$;
- Since the usage of HSRDs aided with an appropriate semi-active control strategy does not increase the base story shear force and structural demand, the HSRDs are an excellent alternative for retrofitting seismic design and strengthening existing buildings in near-field earthquake zones.

REFERENCES

[1] Xu Z, Agrawal AK, He WL, Tan P. (2007). "Performance of passive energy dissipation systems during near-field ground motion type pulses." *Engineering Structures*, 29(2): 224–236.

[2] Symans MD, Constantinou MC. (1999). "Semi-active control systems for seismic protection of structures: a state-of-the-art review." *Engineering Structures*, 21: 469–487.

[3] Leavitt J, Jabbari F, Bobrow JE. (2007). "Optimal performance of variable stiffness devices for structural control." *Journal of Dynamic Systems, Measurement, and Control*, 129(2): 171–177.
[4] Kobori T, Takahashi M, Nasu T, Niwa N, Ogasawara K. (1993). "Seismic response controlled structure with active variable stiffness system." *Earthquake Engineering and Structural Dynamics*, 22(11): 925–941.
[5] Bobrow JE, Jabbari F, Thai K. (1995). "An active truss element and control law for vibration suppression." *Smart Materials and Structures*, 4(4): 264–269.
[6] Bobrow JE, Jabbari F, Thai K. (2000). "A new approach to shock isolation and vibration suppression using a resetable actuator." *Journal of Dynamic Systems, Measurement, and Control*, 122: 570–573.
[7] Bobrow JE, Jabbari F. (1997). "A high-performance semi-active controler for structural vibration supresion." *Smart Structures and Materials*, *SPIE 1997*, 3041: 67–74.
[8] Jabbari F, Bobrow JE. (2002). "Vibration suppression with resettable device." *Journal of Engineering Mechanics*, 128(9): 916–924.
[9] Hazaveh NK, Rad AA, Rodgers GW, Chase JG, Pampanin S, Ma QT. (2017). "Shake table test a structure retrofitted using 2-4 Direction Displacement Dependent (D3) viscous dampers." In *Proceedings of the 2017 NZSEE Conference*. Wellington, New Zealand.
[10] Yang JN, Agrawal AK. (2002). "Semi-active hybrid control systems for nonlinear buildings against near-field earthquakes." *Engineering Structures*, 24: 271–280.
[11] Lu LY, Lin GL. (2009). "Improvement of near-fault seismic isolation using a resettable variable stiffness damper." *Engineering Structures*, 31(9): 2097–2114.
[12] Keyhani A, Sajjadi Alehashem SM, Ni YQ. (2013). "Fabrication and experiment of a hydro-pneumatic semi-active resettable device." *Asian Journal of Civil Engineering (BHRC)*, 14(1): 47–70.
[13] Norouzi M, Sajjadi Alehashem SM, Vatandoost H, Ni YQ, Shahmardan MM. (2016). "A new approach for modeling of magnetorheological elastomers." *Journal of Intelligent Material Systems and Structures*, 27(8): 1121–1135.
[14] Sajjadi Alehashem, S. M., Wang, J., Ni, Y. Q., & Keyhani, A. (2022). "Vibration control of structures against near-field earthquakes by using a novel hydro-pneumatic semi-active resettable device." *Structural Control and Health Monitoring*, 29(11), e3054.
[15] Ashtiani M, Hashemabadi SH, Ghaffari A. (2015). "A review on the magnetorheological fluid preparation and stabilization." *Journal of Magnetism and Magnetic Materials*, 374: 716–730.
[16] Mulligan KJ, Chase JG, Mander JB, Rodgers GW, Elliott RB, Franco-Anaya R, Carr AJ. (2009). " Experimental validation of semi-active resetable actuators in a ⅕th scale test structure." *Earthquake Engineering and Structural Dynamics*, 38(4): 517–536.
[17] Permanent Committee of Revising the Code of Practice for Seismic Resistant Design of Buildings (2014). *Iranian Code of Practice for Seismic Resistant Design of Building (Standard No. 2800), 4th Ed.* Prepared by Building & Housing Research Center, Iran.
[18] Somerville P, Smith N, Punyamurthula S, Sun J. (1997). *Development of ground motion time histories for phase II of the FEMA/SAC steel project.* Report No. SAC/BD-97/04, SAC Background Document Report.